AD-A063 796 AIR FORCE MATERIALS LAB WRIGHT-PATTERSON AFB OHIO F/G 11/4
REPRESENTATION OF MATRIX/INTERFACE-CONTROLLED STRENGTH OF UNIDI--ETC(U)
AUG 78 H T HAHN, J ERIKSON
UNCLASSIFIED AFML-TR-78-85 NL

| OF |
AD
A063796

END
DATE
FILMED
3-79
DDC

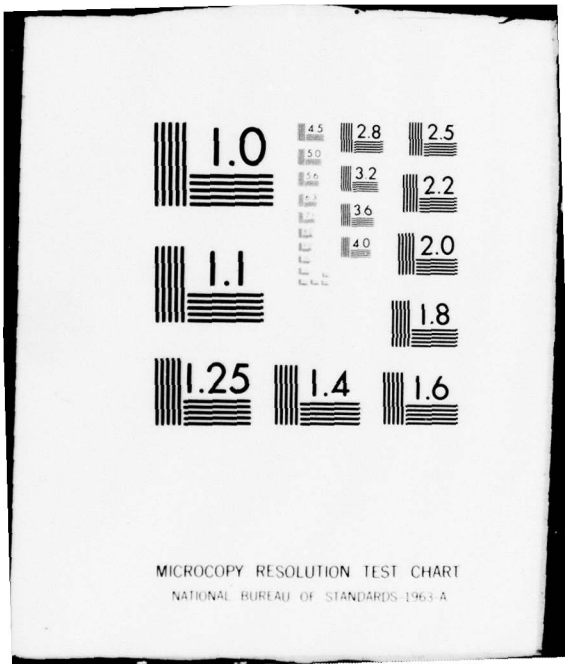
1.0
1.1
1.25
1.4
1.6
1.8
2.0
2.2
2.5
2.8
3.2
3.6
4.0
4.5
5.0
MICROCOPY RESOLUTION TEST CHART
NATIONAL BUREAU OF STANDARDS-1963-A

AFML-TR-78-85

LEVEL II

REPRESENTATION OF MATRIX/INTERFACE-CONTROLLED STRENGTH OF UNIDIRECTIONAL COMPOSITES

AUGUST 1978

TECHNICAL REPORT AFML-TR-78-85
Final Report for Period 1 May 1976 – 31 December 1977

AIR FORCE MATERIALS LABORATORY
AIR FORCE WRIGHT AERONAUTICAL LABORATORIES
AIR FORCE SYSTEMS COMMAND
WRIGHT-PATTERSON AIR FORCE BASE, OHIO 45433

NOTICE

When Government drawings, specifications, or other data are used for any purpose other than in connection with a definitely related Government procurement operation, the United States Government thereby incurs no responsibility nor any obligation whatsoever; and the fact that the government may have formulated, furnished, or in any way supplied the said drawings, specifications, or other data, is not to be regarded by implication or otherwise as in any manner licensing the holder or any other person or corporation, or conveying any rights or permission to manufacture, use, or sell any patented invention that may in any way be related thereto.

This report has been reviewed by the Information Office (ASD/OIP) and is releasable to the National Technical Information Service (NTIS). At NTIS, it will be releasable to the general public, including foreign nations.

This technical report has been reviewed and is approved for publication.

H. THOMAS HAHN
Project Engineer

STEPHEN W. TSAI, Chief
Mechanics & Surface Interactions Branch

FOR THE DIRECTOR

JEROME M. KELBLE, Chief
Nonmetallic Materials Division

Copies of this report should not be returned unless return is required by security considerations, contractual obligations, or notice on a specific document.

AIR FORCE/56780/12 January 1979 — 200

UNCLASSIFIED

SECURITY CLASSIFICATION OF THIS PAGE (When Data Entered)

REPORT DOCUMENTATION PAGE	READ INSTRUCTIONS BEFORE COMPLETING FORM
1. REPORT NUMBER: AFML-TR-78-85	2. GOVT ACCESSION NO.
3. RECIPIENT'S CATALOG NUMBER	
4. TITLE (and Subtitle): REPRESENTATION OF MATRIX/INTERFACE-CONTROLLED STRENGTH OF UNIDIRECTIONAL COMPOSITES.	5. TYPE OF REPORT & PERIOD COVERED: Final Report 1 May 1976-31 Dec 1977
	6. PERFORMING ORG. REPORT NUMBER
7. AUTHOR(s): H. Thomas Hahn, J. Erikson	8. CONTRACT OR GRANT NUMBER(s): INHOUSE
9. PERFORMING ORGANIZATION NAME AND ADDRESS: Air Force Materials Laboratory, Air Force Wright Aeronautical Laboratories, AFSC, Wright-Patterson AFB, Ohio 45433	10. PROGRAM ELEMENT, PROJECT, TASK AREA & WORK UNIT NUMBERS: 62102F 2419 241903 24190310
11. CONTROLLING OFFICE NAME AND ADDRESS: Air Force Materials Laboratory (AFML/MBM), Air Force Wright Aeronautical Laboratories, Wright-Patterson AFB, Ohio 45433	12. REPORT DATE: AUGUST 1978
	13. NUMBER OF PAGES: 36
14. MONITORING AGENCY NAME & ADDRESS (if different from Controlling Office): 38p.	15. SECURITY CLASS. (of this report): Unclassified
	15a. DECLASSIFICATION/DOWNGRADING SCHEDULE

16. DISTRIBUTION STATEMENT (of this Report)

Approved for public release, distribution unlimited.

17. DISTRIBUTION STATEMENT (of the abstract entered in Block 20, if different from Report)

18. SUPPLEMENTARY NOTES

19. KEY WORDS (Continue on reverse side if necessary and identify by block number)

Failure envelope, Fracture toughness, Strength distribution, Inherent crack, Energy release rate, Fracture mechanics, Combined loading

20. ABSTRACT (Continue on reverse side if necessary and identify by block number)

The report presents a method of characterizing the matrix/interface-controlled strength, including scatter, of unidirectional composites under combined loading. The failure envelope is represented by a second order polynomial and the scatter is described by the strength vector whose magnitude has a Weibull distribution. The method is based on the assumption of failure originating at inherent cracks parallel to the fibers and holds promise as a

→over

DD FORM 1 JAN 73 1473 EDITION OF 1 NOV 65 IS OBSOLETE

UNCLASSIFIED

SECURITY CLASSIFICATION OF THIS PAGE (When Data Entered)

20. means of accounting for the size effect under combined loading. In addition, the energy release rate approach is discussed as a physical model and the appropriate data are presented.

FOREWORD

This report describes an inhouse effort conducted in the Mechanics and Surface Interactions Branch (MBM), Nonmetallic Materials Division (MB), Air Force Materials Laboratory, Air Force Wright Aeronautical Laboratories, Wright-Patterson AFB, Ohio, under Project 2419, "Nonmetallic Structural Materials", Task 241903, "Composite Materials and Mechanics Technology", Work Unit 23190310, "Durability of Composites and Adhesives."

The work reported herein was performed during the period 1 May 1976 to 31 December 1977. Dr. H. Thomas Hahn (AFML/MBM) was the project engineer and Dr. J. Erikson was a visiting scientist from the National Defense Research Institute, Stockholm, Sweden, for the period 15 June 1976 to 31 August 1976.

The authors wish to acknowledge R. Esterline and R. Cornwell of the University of Dayton Research Institute for the preparation and testing of composite tubular specimens.

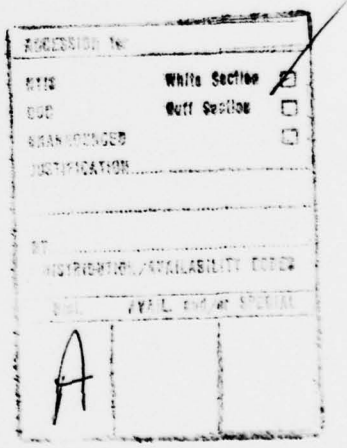

TABLE OF CONTENTS

SECTION		PAGE
I	INTRODUCTION	1
II	PHYSICAL BACKGROUND	3
	1. Interrelationship Between Strength and Fracture Toughness	3
	2. Application of Energy Release Rate Approach	6
	3. Derivation of Strength Distribution from Crack Length Distribution	10
III	ANALYSIS OF COMBINED LOADING DATA	13
	1. Characterization of Strength	13
	2. Size Effect	16
IV	CONCLUSIONS	18
	REFERENCES	19

LIST OF ILLUSTRATIONS

FIGURE		PAGE
1	Composite Lamina with a Through-the-Thickness Crack	26
2	Interaction Between k_2' and k_6'	27
3	Linearized Plot of s	28
4	Distribution of s Based on Censored Data	29
5	Predicted Failure Envelope and Experimental Data for Short Tubes	30

LIST OF TABLES

TABLE		PAGE
1	Strength and Fracture Properties of Scotchply 1002	21
2	Elastic Properties	22
3	Strength Ratios	23
4	Values of a	24
5	Stress Components at Failure	25

SECTION I
INTRODUCTION

Many theories are available for representation of the strengths of unidirectional composites, as surveyed in [1] and [2]. As regards the matrix/interface-controlled strength, which is the topic of discussion in the present report, these theories can be classified by the degree of interaction between the normal and shear stresses and also between tension and compression. For example, the modified von Mises-Hill criterion [1] takes into account the coupling between the transverse normal and shear stresses; however, it requires a different polynomial when the transverse stress is compressive. The maximum stress or maximum strain criterion incorporates no coupling at all; it is based on the independence of the failure modes. The tensor polynomial criterion [1], however, recognizes full coupling and employs only one polynomial.

All of the theories have their advantages and disadvantages. However, one or all of the following three factors can be cited as a reason for preferring one theory to the others: physical foundation, goodness of fit with the data, and convenience.

In most cases, the goodness of fit tests have been performed on the off-axis strength without much success; the off-axis strength decreases rapidly with increasing off-axis angle, thus contributing to the possiblity of visual deception in graphical comparisons. Consequently, it is difficult to distinguish one theory from another graphically.

Convenience depends on the type of application. For example, the tensor polynomial criterion is simpler in digital applications whereas the maximum strain criterion is more convenient in graphical applications.

As for the physical foundations behind the failure theories, one may observe that the von Mises-Hill criterion assumes failure to be independent of hydrostatic stress and that the maximum stress or maximum strain

criterion is based on the noninteraction among the failure modes. However, no physical foundation has been provided for the tensor polynomial criterion.

The objective of the present report is to discuss some of the physical evidences in support of the tensor polynomial criterion and propose a corresponding characterization procedure for the combined loading strength including scatter. The discussion is limited only to unidirectional polymer matrix composites subjected to transverse normal and longitudinal shear stresses so that composite failure is controlled by the matrix/interface properties. Thus the appropriate polynomial is of the form

$$F_2\sigma_2 + F_{22}\sigma_2^2 + F_{66}\sigma_6^2 = 1$$

The foregoing polynomial follows from the more general tensor polynomial in [1] in the absence of the longitudinal stress in the fiber direction, σ_1. However, recognizing the difference between the fiber-controlled failure and the matrix/interface-controlled failure, we propose that the reduced polynomial be used to describe the matrix/interface-controlled strength even when $\sigma_1 \neq 0$. It goes without saying that the fiber-controlled strength is then described by

$$F_1\sigma_1 + F_{11}\sigma_1^2 = 1 \ .$$

SECTION II

PHYSICAL BACKGROUND

1. INTERRELATIONSHIP BETWEEN STRENGTH AND FRACTURE TOUGHNESS

Just like homogeneous brittle materials, unidirectional composites exhibit, when the artificially introduced crack is parallel to the fibers [3], those fracture characteristics that are amenable to the linear elastic fracture mechanics predictions. In addition, the transverse or shear strength of unnotched composite is known to depend strongly on the inherent defects such as voids and interfacial debonds [4, 5, 6]. Thus, if these defects are regarded as typical cracks, the unnotched strength can be predicted from the fracture toughness and the size of the defect [7, 8].

Suppose the unnotched strength is represented by the polynomial,

$$F_2\sigma_2 + F_{22}\sigma_2^2 + F_{66}\sigma_6^2 = 1 \tag{1}$$

where σ_2 is the transverse normal stress and σ_6 the longitudinal shear stress. The F's are the components of strength tensors.

Now, if the failure is assumed to initiate at an inherent crack of half length a_o parallel to the fibers, Figure 1, Equation (1) can be rewritten in terms of the nominal stress intensity factors k'_2, k'_6

$$A_2k'_2 + A_{22}k'^2_2 + A_{66}k'^2_6 = 1 \tag{2}$$

where

$$k'_2 = \sigma_2\sqrt{a_o} \tag{3}$$

$$k'_6 = \sigma_6\sqrt{a_o} \tag{4}$$

The parameters A's are related to the F's through

$$A_2 = F_2/\sqrt{a_o}, \tag{5}$$

$$A_{22} = F_{22}/a_o, \tag{6}$$

$$A_{66} = F_{66}/a_o \tag{7}$$

In the foregoing derivation, the surface of the inherent crack is not necessarily normal to σ_2, Figure 1. However, when σ_2 is tensile, the inherent crack can be assumed normal to σ_2 and the nominal stress intensity factors, k_2', k_6', reduce to the mode I and mode II stress intensity factors, k_1, k_2, respectively. Consequently, Equation (2) can be considered in the first quadrant as representing a mixed-mode fracture toughness envelope under in-plane loadings. Moreover, through the use of the uniaxial strengths and corresponding fracture toughnesses, a_o can be determined from

$$a_o = \left(\frac{k_{1c}}{X_2}\right)^2 \tag{8}$$

or

$$a_o = \left(\frac{k_{2c}}{X_6}\right)^2 \tag{9}$$

where X_2 and X_6 are the transverse tensile and shear strengths, respectively, and k_{1c} and k_{2c} are the mode I and mode II fracture toughnesses, respectively.

The foregoing hypothesis can be checked against the data for Scotchply 1002. The appropriate strength and fracture properties are listed in Table 1 [9]. The inherent crack half length is then

$$a_o = 2.61 \text{ mm} \quad \text{or} \quad 3.53 \text{ mm} \tag{10}$$

depending on whether Equation (8) or (9) is used.

There are many factors that can contribute to the difference in the calculated values of a_o: test method, material variability, and the assumption of through-the-thickness crack. Although effects of the last two factors cannot

be clearly defined at present, the first seems to point in the right direction. That is, k_{2c} was determined from a cantilever beam subjected to a concentrated load [3]. Since this test is closer to the short beam shear test than to the off-axis tension, the interlaminar strength should be used for X_6. Since the interlaminar shear strength is usually higher than the inplane shear strength that was used in Equation (9), the resulting a_o will be smaller than 3.53 mm and hence closer to what is predicted by Equation (8).

For the foregoing reasons and also since the overall comparison between the strength and fracture toughness under combined stress is of interest, we take the average value

$$a_o = 3.07 \text{ mm} \tag{11}$$

and proceed to investigate the consequences. The fracture toughness tensor components follow upon substitution of the F's in Table 1 and a_o into Equations (5) and (7):

$$A_2 = 0.7735 \quad (\text{MNm}^{-3/2})^{-1} \tag{12}$$

$$A_{22} = 0.1179 \quad (\text{MNm}^{-3/2})^{-2} \tag{13}$$

$$A_{66} = 0.07459 \quad (\text{MNm}^{-3/2})^{-2} \tag{14}$$

The resulting fracture toughness envelope is seen to agree well, in the first quadrant, with the experimental data in Figure 2. It should be noted that the data were obtained from the artificially introduced cracks which are normal to σ_2 [3].

The mode II fracture toughness increases as transverse compression is applied because of the friction between the crack surfaces [9]. This increase is correctly, although lacking in quantitative accuracy, predicted by the polynomial strength criterion,but not by the other criteria. Also, the coupling between k_2' and k_6' in the first quadrant can be described neither by

the maximum stress criterion nor by the maximum strain criterion.

Thus, it can be concluded that the polynomial strength criterion agrees, when the transverse stress is tensile, with the basic characteristics of the available fracture toughness envelope. As the transverse compression increases, however, the failure will in general start from an inherent crack whose surfaces are inclined to the applied stress. How this critical angle of inclination depends on the applied stresses should be known if the entire failure envelope is to be related to the fracture toughness. By way of illustrating this dependency, we discuss the energy release rate approach in the following subsection.

2. APPLICATION OF ENERGY RELEASE RATE APPROACH

Since the crack extension in unidirectional composites is at least macroscopically self-similar, the energy release rate can be calculated easily. That is, for a crack parallel to the fibers, the total energy release rate becomes [10]

$$G = G_1 + G_2 + G_3 \tag{15}$$

Here the energy release rates G_1, G_2, G_3 resulting from k_1, k_2 and k_3, respectively, are given by

$$G_1 = \pi B_1 k_1^2 , \qquad B_1 = a \frac{1}{E_T} \tag{16}$$

$$G_2 = \pi B_2 k_2^2 , \qquad B_2 = B_1 \left(\frac{E_T}{E_L} \right)^{1/2} \tag{17}$$

$$G_3 = \pi B_3 k_3^2 , \qquad B_3 = \frac{1}{2(G_{TT} G_{LT})^{1/2}} \tag{18}$$

Note that k_3 is the mode III stress intensity factor. The orthotropy correction factor a is defined by

$$a = \frac{1}{\sqrt{2}}\left[\left(\frac{E_T}{E_L}\right)^{1/2} + \frac{E_T/G_{LT} - 2\nu_{TL}}{2}\right]^{1/2} \tag{19}$$

where E_L is the longitudinal modulus parallel to the fibers, E_T the transverse modulus, ν_{TL} the minor Poisson's ratio, G_{LT} the longitudinal shear modulus, and G_{TT} the transverse shear modulus.

We now consider a crack of length $2a_o$ which is not normal to σ_2 but inclined by an angle θ, Figure 1. In terms of the applied stresses σ_2 and σ_6, the stress intensity factors for this crack are expressed as follows:

$$k_1 = \sigma_2\sqrt{a_o}\cos^2\theta \quad , \quad \sigma_2 \geq 0 \tag{20}$$

$$k_1 = 0 \quad , \quad \sigma_2 < 0 \tag{21}$$

$$k_2 = \sigma_6\sqrt{a_o}\cos\theta \tag{22}$$

$$k_3 = \sigma_2\sqrt{a_o}\sin\theta\cos\theta \tag{23}$$

Note that in the calculation of k_3 no friction has been taken into account.

When σ_2 is positive, G becomes stationary, i.e., $dG/d\theta = 0$, at the following angles:

$$\theta = 0 \text{ or } \pi/2 \tag{24}$$

$$\theta = \sin^{-1}\left[\frac{1}{2} - \frac{B_1 + B_2(\sigma_6/\sigma_2)^2}{2(B_3 - B_1)}\right]^{1/2} \tag{25}$$

On the other hand, if σ_2 is negative, then $G_1 = 0$ and the angle given by Equation (25) is changed to

$$\theta = \sin^{-1}\left[\frac{1}{2} - \frac{B_2}{2B_3}\left(\frac{\sigma_6}{\sigma_2}\right)^2\right]^{1/2} \tag{26}$$

Elastic properties of commonly used composites are listed in Table 2 together with the calculated values of B's. For those composites, we have

$$2B_1 > B_3 \tag{27}$$

and therefore Equation (25) cannot be satisfied. Thus, when σ_2 is tensile, the maximum energy release rate occurs at $\theta = 0$ independently of the shear stress σ_6 and

$$G_{max} = G\Big|_{\theta=0} = \pi a_o(B_1\sigma_2^2 + B_2\sigma_6^2) \tag{28}$$

However, when σ_2 is compressive, the critical crack orientation depends on the stress ratio σ_6/σ_2. That is, if $\left|\sigma_6/\sigma_2\right| \geq (B_3/B_2)^{1/2}$, then

$$G_{max} = G\Big|_{\theta=0} = \pi a_o B_2 \sigma_6^2 \tag{29}$$

On the other hand, if $\left|\sigma_6/\sigma_2\right| < (B_3/B_2)^{1/2}$, then

$$G_{max} = G\Big|_{\theta=\theta_o} = \pi a_o B_2 \sigma_6^2 \left[\frac{1}{2} + \frac{1}{4}\frac{B_3}{B_2}\left(\frac{\sigma_2}{\sigma_6}\right)^2 + \frac{1}{4}\frac{B_2}{B_3}\left(\frac{\sigma_6}{\sigma_2}\right)^2\right] \tag{30}$$

where θ_o satisfies Equation (26). Note that, when $\sigma_6=0$, i.e., pure compression, one obtains

$$\theta_o = \pi/4 \tag{31}$$

and

$$G_{max} = \pi a_o B_3 \sigma_2^2/4 \tag{32}$$

If the energy release rate is applicable, the uniaxial strengths are related to the critical energy release rate G_c by

$$X_6 = \left(\frac{G_c}{\pi a_o B_2}\right)^{1/2} \tag{33}$$

$$\frac{X_2}{X_6} = \left(\frac{B_2}{B_1}\right)^{1/2} \tag{34}$$

$$\frac{X_2'}{X_6} = 2\left(\frac{B_2}{B_3}\right)^{1/2} \tag{35}$$

where X_2' is the compressive transverse strength. The combined-stress failure criteria then follows from Equations (28)-(30). That is, when $\sigma_2 \geq 0$, Equation (28) reduces to

$$\left(\frac{\sigma_2}{X_2}\right)^2 + \left(\frac{\sigma_6}{X_6}\right)^2 = 1 \tag{36}$$

When $\sigma_2 < 0$, on the other hand, two different criteria follow depending on the ratio $|\sigma_6/\sigma_2|$. If $|\sigma_6/\sigma_2| > (B_3/B_2)^{1/2}$, then the shear strength is independent of σ_2, i.e.

$$\sigma_6 = X_6 \tag{37}$$

However, if $|\sigma_6/\sigma_2| < (B_3/B_2)^{1/2}$, then the failure criterion is given by

$$\left(\frac{\sigma_2}{X_2'}\right)^2 + \left(\frac{\sigma_6}{X_6}\right)^2\left[\frac{1}{2} + \frac{1}{16}\left(\frac{X_2'}{X_6}\right)^2\left(\frac{\sigma_6}{\sigma_2}\right)^2\right] = 1 \tag{38}$$

Table 3 lists the appropriate strength ratios for various composites, both experimental and predicted. Insofar as the ratio X_2/X_6 is concerned, the energy release rate approach seems to yield a fairly good correlation with the data for both graphite/epoxy composites. However, the correlation is very poor for the ratio X_2'/X_6 irrespectively of the type of material.

In any case, the energy release rate implies a strong interaction between σ_2 and σ_6. Aside from the applicability of the energy release rate approach, there are many assumptions, such as the noninteracting through-the-thickness cracks, the mode III fracture in compression, etc., that have

to be validated in order to account for the discrepancy between the theory and the data. Still, what is interesting is that the dependence on the inherent crack length of the strength under combined stresses simply follows from the failure envelope if σ_2 and σ_6 are replaced by $\sigma_2\sqrt{a_o}$ and $\sigma_6\sqrt{a_o}$, respectively. Thus, it is plausible to assume that Equations (1) through (7) are valid in the entire σ_2-σ_6 space and that the A's are independent of a_o.

3. DERIVATION OF STRENGTH DISTRIBUTION FROM CRACK LENGTH DISTRIBUTION

Now that the relationship between the strength and the inherent crack length is known, we can derive a strength distribution under combined loading. To this end we further note that the critical crack orientation is independent of the crack length, as shown in the preceding subsection. Thus, we can assume that the scatter in strength is solely due to the variation in the crack length.

Suppose the crack half length has the cumulative distribution

$$P(a) = \exp\left[-\left(\frac{\hat{a}}{a}\right)^{\alpha/2}\right] \tag{39}$$

where $\hat{a}$ and α are the characterization parameters. Since the A's in Equations (5) - (7) can be considered as deterministic material constants, we obtain the following distributions of F's:

$$P(F_2) = \exp\left[-\left(\frac{\hat{F}_2}{F_2}\right)^{\alpha}\right] \tag{40}$$

$$P(F_{22}) = \exp\left[-\left(\frac{\hat{F}_{22}}{F_{22}}\right)^{\alpha/2}\right] \tag{41}$$

$$P(F_{66}) = \exp\left[-\left(\frac{\hat{F}_{66}}{F_{66}}\right)^{\alpha/2}\right] \tag{42}$$

where $\hat{F}$'s correspond to $\hat{a}$ through Equations (5) - (7).

We now introduce the concept of a strength vector [9]. Suppose failure occurs at the stresses σ_2 and σ_6. The pair (σ_2, σ_6) then defines, in the stress space, a vector which is called the strength vector. Since the failure envelope represents a set of pairs of failure stresses, any point on the failure envelope has a strength vector associated with it. From Equations (1) and (5)-(7), the magnitude σ of this strength vector (σ_2, σ_6), called the combined strength hereafter, is shown to be proportional to $1/\sqrt{a}$:

$$\sigma = \frac{\left[(A_2^2 + 4A_{22})\cos^2\phi + 4A_{66}\sin^2\phi\right]^{1/2} - A_2\cos\phi}{2(A_{22}\cos^2\phi + A_{66}\sin^2\phi)} \quad \frac{1}{\sqrt{a}} \tag{43}$$

where

$$\phi = \tan^{-1}(\sigma_6/\sigma_2) \tag{44}$$

Then, introducing the characteristic combined strength,

$$\hat{\sigma} = \sigma\Big|_{a=\hat{a}} \tag{45}$$

we can rewrite Equation (43) as

$$\frac{\sigma}{\hat{\sigma}} = \left(\frac{\hat{a}}{a}\right)^{1/2} \tag{46}$$

Therefore, the probability of the combined strength being greater than σ, $R(\sigma)$, is expressed in the following simple form:

$$R(\sigma) = \exp\left[-\left(\frac{\sigma}{\hat{\sigma}}\right)^{\alpha}\right] \tag{47}$$

Note that the characteristic combined strength $\hat{\sigma}$ varies with the angle ϕ. However, the distribution of the ratio $\sigma/\hat{\sigma}$ remains independent of ϕ. Also, $\sigma/\hat{\sigma}$ has the same distribution as do the uniaxial strengths. In fact, Equation (47) reduces to

$$R(X_2) = \exp\left[-\left(\frac{X_2}{\hat{X}_2}\right)^{\alpha}\right] \tag{48}$$

$$R(X_2') = \exp\left[-\left(\frac{X_2'}{\hat{X}_2'}\right)^{\alpha}\right] \tag{49}$$

for the tensile and compressive transverse strengths, respectively, and to

$$R(X_6) = \exp\left[-\left(\frac{X_6}{\hat{X}_6}\right)^{\alpha}\right] \tag{50}$$

for the shear strength.

As is clear by now, the shape parameter α is independent of the mode of loading. Table 4 lists values of α for some composites available in the literature. No definitive relationship is seen between α and the mode of loading although some of the inconsistencies may be due to the difference in the test methods employed. Therefore, in the following section, we assume α is independent of the type of loading and adopt the procedure based on σ to characterize the combined strength data.

SECTION III
ANALYSIS OF COMBINED LOADING DATA

1. CHARACTERIZATION OF STRENGTH

Strength data were obtained by testing off-axis tubes in combined axial and torsional loadings. The experimental procedures are described in [17].

The strengths listed in Table 5 are fit by the equation

$$F_{o2}\sigma_2 + F_{o22}\sigma_2^2 + F_{o66}\sigma_6^2 = 1 \tag{51}$$

where F_o's are determined by the least squares method. That is, Equation (51) for each set of data $(\sigma_2^{(i)}, \sigma_6^{(i)})$, is rearranged as follows

$$\begin{bmatrix} \sigma_2^{(1)} & \sigma_2^{(1)^2} & \sigma_6^{(1)^2} \\ \sigma_2^{(2)} & \sigma_2^{(2)^2} & \sigma_6^{(2)^2} \\ - & - & - \\ \sigma_2^{(n)} & \sigma_2^{(n)^2} & \sigma_6^{(n)^2} \end{bmatrix} \begin{Bmatrix} F_{o2} \\ F_{o22} \\ F_{o66} \end{Bmatrix} = \begin{Bmatrix} 1 \\ 1 \\ - \\ 1 \end{Bmatrix} \tag{52}$$

Using an abridged notation for Equation (52), i.e.

$$[\sigma]\{F_o\} = \{1\}, \tag{53}$$

we can determine F_o's from the following equation:

$$\{F_o\} = ([\sigma]^T[\sigma])^{-1}[\sigma]^T\{1\} \tag{54}$$

where the subscripts T and -1 stand for the transpose and inversion, respectively. The results are

$$F_{o2} = 3.376 \times 10^{-2} \text{ (MPa)}^{-1} \tag{55}$$

$$F_{o22} = 4.721 \times 10^{-4} \text{ (MPa)}^{-2} \tag{56}$$

$$F_{o66} = 2.384 \times 10^{-4} \text{ (MPa)}^{-2} \tag{57}$$

Next, in order to determine $\hat{F}$'s, a nondimensional strength parameter s is defined by

$$s = \sigma/\sigma_o \tag{58}$$

where σ is the actual combined strength and σ_o is the combined strength predicted by the failure envelope, Equation (51). That is, if (σ_2, σ_6) is a pair of stress components at failure, then

$$\sigma = \left(\sigma_2^2 + \sigma_6^2\right)^{1/2} \tag{59}$$

$$\sigma_o = \left(\sigma_{o2}^2 + \sigma_{o6}^2\right)^{1/2} \tag{60}$$

where $(\sigma_{o2}, \sigma_{o6})$ satisfies Equation (51) and

$$\frac{\sigma_2}{\sigma_{o2}} = \frac{\sigma_6}{\sigma_{o6}} = s \tag{61}$$

Recalling that σ has a Weibull distribution, Equation (47), we deduce

$$R(s) = \exp\left[-\left(\frac{s}{\hat{s}}\right)^{\alpha}\right], \quad \hat{s} = \frac{\hat{\sigma}}{\sigma_o} \tag{62}$$

The experimental values of s are plotted in Figure 3 according to the linearized format of Equation (62);

$$\ell n(-\ell nR) = \alpha \ell n\, s - \alpha \ell n\, \hat{s} \tag{63}$$

The median rank was used for R:

$$R = 1 - \frac{j - 0.3}{N + 0.4} \tag{64}$$

where j is the ordinal number of strength and N the total number of data.

The data represented by the closed symbols are seen to deviate much from the trend exhibited by the open symbols. Two of those four data were obtained from badly misaligned 15-degree off-axis tubes; therefore, these can be regarded as invalid data. The remaining two did not exhibit any apparent anomalies. However, it is still possible that a slight misalignment may have caused premature failure since these two are 90-degree tubes.

Therefore, the aforementioned four points are discarded and new F_os are calculated with the results

$$F_{o2} = 3.126 \times 10^{-2} \quad (\text{MPa})^{-1} \tag{65}$$

$$F_{o22} = 4.428 \times 10^{-4} \quad (\text{MPa})^{-2} \tag{66}$$

$$F_{o66} = 2.391 \times 10^{-4} \quad (\text{MPa})^{-2} \tag{67}$$

The distribution of s based on the newly determined F_o's is shown in Figure 4. The best-fit curve results from

$$\alpha = 4.745 \quad , \quad \hat{s} = 0.9695 \tag{68}$$

and the correlation coefficient is 0.9922. Furthermore, the corresponding $\hat{F}$'s are obtained from the following equations:

$$\frac{F_{o2}}{\hat{F}_2} = \hat{s} \tag{69}$$

$$\frac{F_{o22}}{\hat{F}_{22}} = \frac{F_{o66}}{\hat{F}_{66}} = \hat{s}^2 \tag{70}$$

Thus, the matrix/interface-controlled strength of the composite studied is characterized by the distribution of σ, Equation (47), and by the $\hat{F}$'s:

$$\hat{F}_2 = 3.224 \times 10^{-2} \quad (\text{MPa})^{-1} \tag{71}$$

$$\hat{F}_{22} = 4.567 \times 10^{-4} \quad (\text{MPa})^{-2} \tag{72}$$

$$\hat{F}_{66} = 2.466 \times 10^{-4} \quad (\text{MPa})^{-2} \tag{73}$$

Now, given any applied stresses, the survival probability can be calculated.

As an example, suppose the following stresses are applied to the previously characterized composite:

$$\sigma_2 = -40 \text{ MPa} \quad , \quad \sigma_6 = 60 \text{ MPa} \tag{74}$$

The stress ratio $\sigma/\hat{\sigma}$ follows from Equations (71)-(73) as

$$\frac{\sigma}{\hat{\sigma}} = 0.779 \tag{75}$$

Thus, the probability of survival, R, is given by

$$R = \exp\left[-(0.779)^{4.745}\right] = 0.737 \tag{76}$$

2. SIZE EFFECT

To see if the weakest link theory based on s can account for the size effect, some data were obtained from 90-degree tubes having gage length reduced to 3/8 the original gage length. Described in the following are the results, both analytical and experimental.

Following the same procedure as, e.g., in [18], but using s, we obtain the ratio of the characteristic strength parameters as

$$\frac{\hat{s}'}{\hat{s}} = \left(\frac{V}{V'}\right)^{1/a} = \left(\frac{8}{3}\right)^{1/4.745} = 1.2296 \tag{77}$$

Here the primed quantities are associated with the short tubes and V is the volume. The $\hat{F}$'s for the short tubes are then

$$\hat{F}_{2'}' = \hat{F}_2 \hat{s}/\hat{s}' = 2.542 \times 10^{-2} \text{ (MPa)}^{-1} \quad (78)$$

$$\hat{F}_{22}' = \hat{F}_{22} \hat{s}/\hat{s}' = 2.939 \times 10^{-4} \text{ (MPa)}^{-2} \quad (79)$$

$$\hat{F}_{66}' = \hat{F}_{66} \hat{s}/\hat{s}' = 1.581 \times 10^{-4} \text{ (MPa)}^{-2} \quad (80)$$

The resulting failure envelope is compared with the experimental results in Figure 5. The broken curve is the best fit of the data. Although any definitive conclusions require more data, the comparison seems quite encouraging.

SECTION IV
CONCLUSIONS

We have presented a method of characterizing the matrix/interface-controlled strength, including scatter, of unidirectional composites under combined transverse normal and shear loading. It was assumed that failure initiates at inherent cracks parallel to the fibers and that the scatter in strength is a manifestation of nonuniform crack length having a certain distribution. The energy release rate approach was discussed as a guide for a possible relationship between the combined strength and the inherent crack length.

The proposed failure criterion is a second order polynomial. The scatter is described by the strength vector whose magnitude has a Weibull distribution. The method holds promise as a means of accounting for the size effect under combined loading.

In the energy release rate approach, actual defects were replaced by the noninteracting through-the-thickness cracks and the critical crack orientation was assumed to depend on the applied stresses in a deterministic manner. The relaxation of the first assumption calls for a three-dimensional stress analysis and the second assumption can be alleviated by employing a statistical approach, as was done for homogeneous materials in [19]. However, a major obstacle to the establishment of a strength-fracture toughness relationship seems to be the lack of an appropriate fracture criterion under combined state of stresses.

REFERENCES

1. E. M. Wu, "Phenomenological Anisotropic Failure Criterion," Composite Materials, Vol. 2, G. P. Sendeckyj, Editor, Academic Press, New York, 1974, p. 353.

2. R. S. Sandhu, A Survey of Failure Theories of Isotropic and Anisotropic Materials, Air Force Flight Dynamics Laboratory, Wright-Patterson Air Force Base, Ohio 45433, AFFDL-TR-72-71, Jan. 1972.

3. E. M. Wu and R. C. Reuter, Jr., Crack Extension in Fiberglass Reinforced Plastics, Univ. of Illinois, T&AM Report No. 275, Feb. 1965.

4. H. T. Corten, "Influence of Fracture Toughness and Flaws on the Interlaminar Shear Strength of Fibrous Composites," Fundamental Aspects of Fiber Reinforced Plastic Composites, R. T. Schwartz and H. S. Schwartz, Editors, Interscience Pub., New York, 1968, p. 89.

5. L. B. Greszczuk, Micromechanics Failure Criteria for Composites, McDonnell Douglas Astronautics Co., Contract No. N00019-72-0221, May 1973.

6. R. D. Vannucci, "Effect of Processing Parameters on Autoclaved PMR Polyimide Composites," Proceedings of the 9th National SAMPE Technical Conference, Vol. 9, SAMPE, Oct. 1977, p. 177.

7. K. Lauraitis, Tensile Strength of Off-Axis Unidirectional Composites, Univ. of Illinois, T&AM Report No. 344, Aug. 1971.

8. G. C. Sih and E. P. Chen, "Fracture Analysis of Unidirectional Composites," Journal of Composite Materials, Vol. 7, 1973, p. 230.

9. E. M. Wu, "Strength and Fracture of Composites," Composite Materials, Vol. 5, L. J. Broutman, Editor, Academic Press, New York, 1974, p. 191.

10. G. C. Sih and H. Liebowitz, "Mathematical Theories of Brittle Fracture," Fracture: An Advanced Treatise, Vol. 2, H. Liebowitz, Editor, Academic Press, New York, 1968, p. 68.

11. K. E. Hofer, Jr., D. Larsen, and V. E. Humphreys, Development of Engineering Data on the Mechanical and Physical Properties of Advanced Composite Materials, Air Force Materials Laboratory, Wright-Patterson Air Force Base, Ohio 45433, AFML-TR-74-266, Feb. 1975.

12. R. M. Verette and J. D. Labor, Structural Criteria for Advanced Composites, Vol. II, Air Force Flight Dynamics Laboratory, Wright-Patterson Air Force Base, Ohio 45433, AFFDL-TR-76-142, Vol. II, March 1977.

13. P.D. Shockey, K. E. Hofer, and D. W. Wright, Structural Airframe Application of Advanced Composite Materials, Vol. IV, Air Force Materials Laboratory, Wright-Patterson Air Force Base, Ohio 45433, AFML-TR-69-101, Vol. IV, Oct. 1969.

14. G. P. Sendeckyj, presented at Mechanics of Composites Review, Dayton, Ohio, Oct. 1977.

15. B. Burroughs, D. Konishi, and M. Nadler, Advanced Composites Serviciability Program, Progress Report No. NA-76-783-2, Rockwell International, Contract No. F33615-76-C-5344, Apr. 1977.

16. G. C. Grimes et al., A Study of the Stress-Strain Behavior of Graphite Fiber Composites to Assess the Stress Levels at Which Significant Damage Occurs, Air Force Materials Laboratory, Wright-Patterson Air Force Base, Ohio 45433, AFML-TR-73-311, Jan. 1974.

17. H. T. Hahn and J. Erikson, Characterization of Composite Laminates Using Tubular Specimens, Air Force Materials Laboratory, Wright-Patterson Air Force Base, Ohio 45433, AFML-TR-77-144, Aug. 1977.

18. M. Knight and H. T. Hahn, "Strength and Elastic Modulus of a Randomly Distributed Short Fiber Composite," Journal of Composite Materials, Vol. 9, 1975, p. 77.

19. S. B. Batdorf and J. G. Crose, "A Statistical Theory for the Fracture of Brittle Structures Subjected to Nonuniform Polyaxial Stresses," Journal of Applied Mechanics, Vol. 41, 1974, p. 459.

TABLE 1

STRENGTH AND FRACTURE PROPERTIES
OF SCOTCHPLY 1002[a]

X_2(MPa)	X_6(MPa)	k_{1c}(MNm$^{-3/2}$)	k_{2c}(MNm$^{-3/2}$)
20.0	66.2	1.022	3.934

F_2 (GPa)$^{-1}$	F_{22} (GPa)$^{-2}$	F_{66} (GPa)$^{-2}$
42.79	360.76	228.24

(a) Data taken from [9]

TABLE 2

ELASTIC PROPERTIES

	Gl/Ep Scotchply 1002	Gr/Ep T300/5208	Gr/Ep AS/3501	B/Ep Narmco 5505
E_L(GPa)	34.47	181.33	137.69	207.53
E_T(GPa)	11.49	10.34	9.65	18.82
G_{LT}(GPa)	4.86	7.17	4.21	5.24
ν_{LT}	0.05	0.28	0.30	0.21
G_{TT}[(a)](GPa)	4.32	3.89	3.63	7.08
$B_1(MPa)^{-1}$	81.24	66.43	86.35	54.16
$B_2(MPa)^{-1}$	46.90	15.86	22.86	16.31
$B_3(MPa)^{-1}$	109.12	94.69	127.88	82.11
Reference	[3]	[11]	[12]	[13]

(a) $G_{TT} = E_T/[2(1 + \nu_{TT})]$, $\nu_{TT} = 0.33$.

TABLE 3

STRENGTH RATIOS

Material	X_2/X_6		X_2'/X_6		X_6	Test Method for Shear
	Exp	Theory	Exp	Theory	(MPa)	
Gl/Ep Scotchply 1002	0.32	0.76	2.22	1.31	66.2	-
Gr/Ep T300/5208	0.60	0.49	3.71	0.82	67.6	[±45] Laminate
Gr/Ep AS/3501-5	0.73	0.52	3.84	0.85	52.1	Rail Shear
B/Ep Narmco 5505	0.98	0.55	4.72	0.89	66.5	[±45] Laminate

TABLE 4

VALUES OF α

Material	Trans. Tension	Trans. Compression	Shear	No. of Specimens	Reference
Gr/Ep					
AS/3501-5	21	26.8	12.6[a]	10	[12]
AS/3501-5	16.9	-	20.9[b]	5-6	[14]
AS/3501-5A	11.3	-	14.6[c]	13-14	[15]
HTS/2256	9.4	5.5	7.4[d]	9-15	[16]
B/Ep					
Narmco 5505	17.5	13.2	12.0[d]	7-15	[13]

(a) Rail Shear
(b) 10-degree off-axis tension
(c) Short beam shear
(d) [±45] laminate tension

TABLE 5

STRESS COMPONENTS AT FAILURE

Spec. No.	σ_1 MPa	σ_2 MPa	σ_6 MPa	Spec. No.	σ_1 MPa	σ_2 MPa	σ_6 MPa
0 - 1	375.4	0	44.38	-45 - 2	97.22	-97.22	0
0 - 2	0	0	48.04	-45 - 3	155.4	-85.81	34.78
0 - 3	-375.4	0	-39.02	-60 - 1	55.60	11.05	51.34
0 - 4	0	0	-48.60	60 - 2	86.56	-34.81	-64.91
15 - 1	-259.4	-18.62	59.50	-60 - 3	116.1	-78.02	78.03
-15 - 1	139.2	9.99	37.30	90 - 1	0	12.82	0
-15 - 2	135.1	-8.03	3.12	90 - 2	0	23.67	0
-15 - 3	323.2	-58.68	-66.20	90 - 2'[a]	0	20.26	0
15 - 3	11.49	4.26	-9.50	90 - 3	0	0	-74.95
-30 - 1	118.4	12.78	45.26	90 - 3'[a]	0	0	-79.36
-30 - 2	193.8	-85.15	-17.79	90 - 4	0	8.04	0
-30 - 3	-11.64	11.61	6.69	90 - 5	0	8.94	0
-45 - 1	-13.79	25.03	5.62	90 - 6	0	0	70.12

(a) Retested after failure.

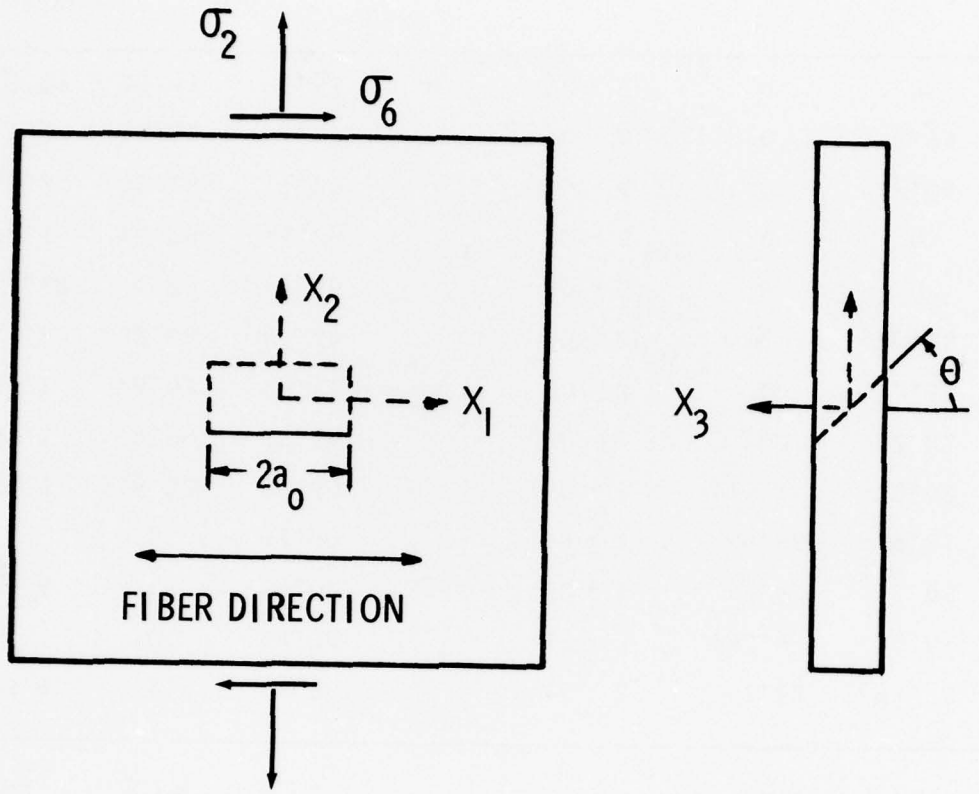

Figure 1. Composite Lamina with a Through-the-Thickness Crack.

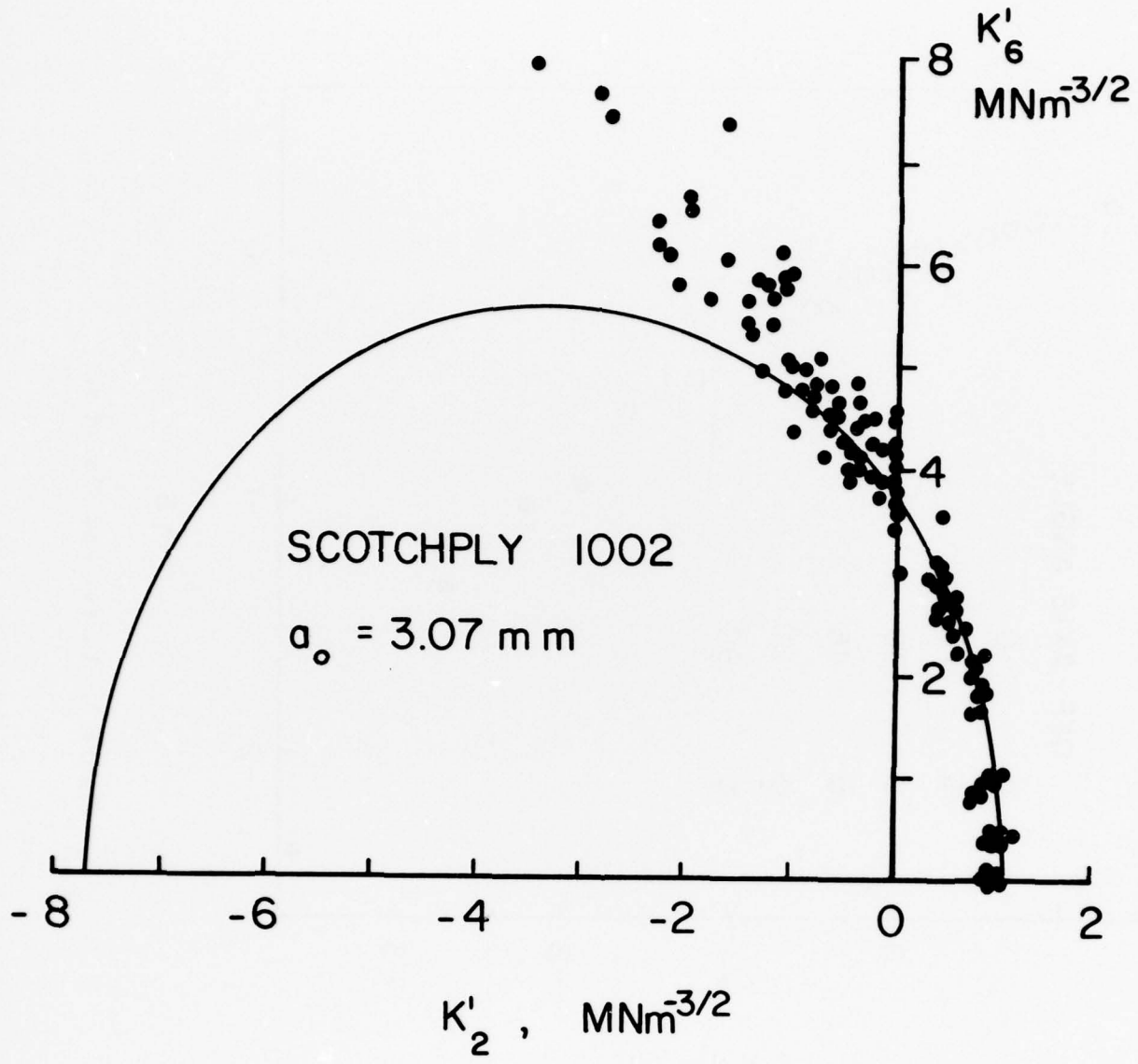

Figure 2. Interaction Between k'_2 and k'_6.

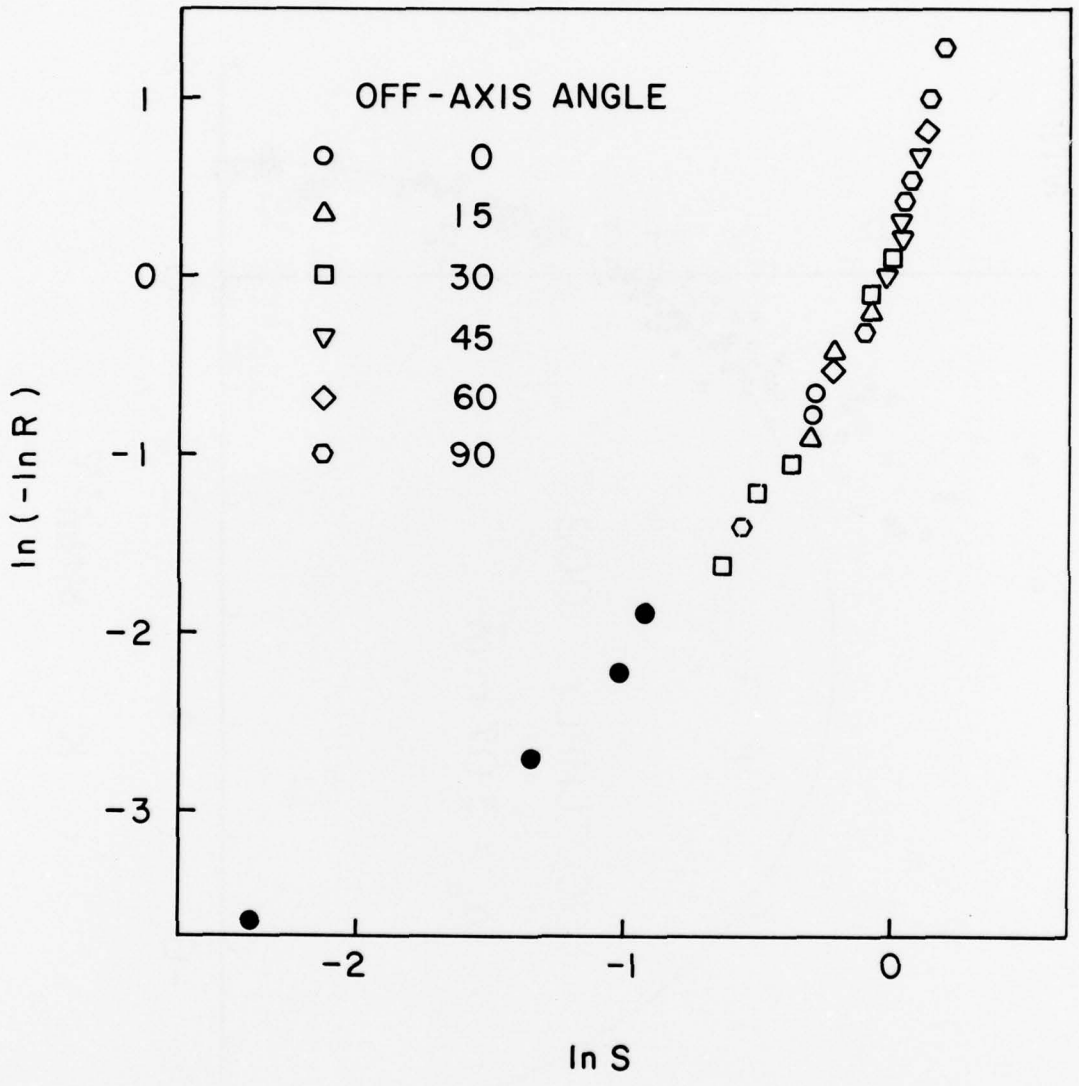

Figure 3. Linearized Plot of s.

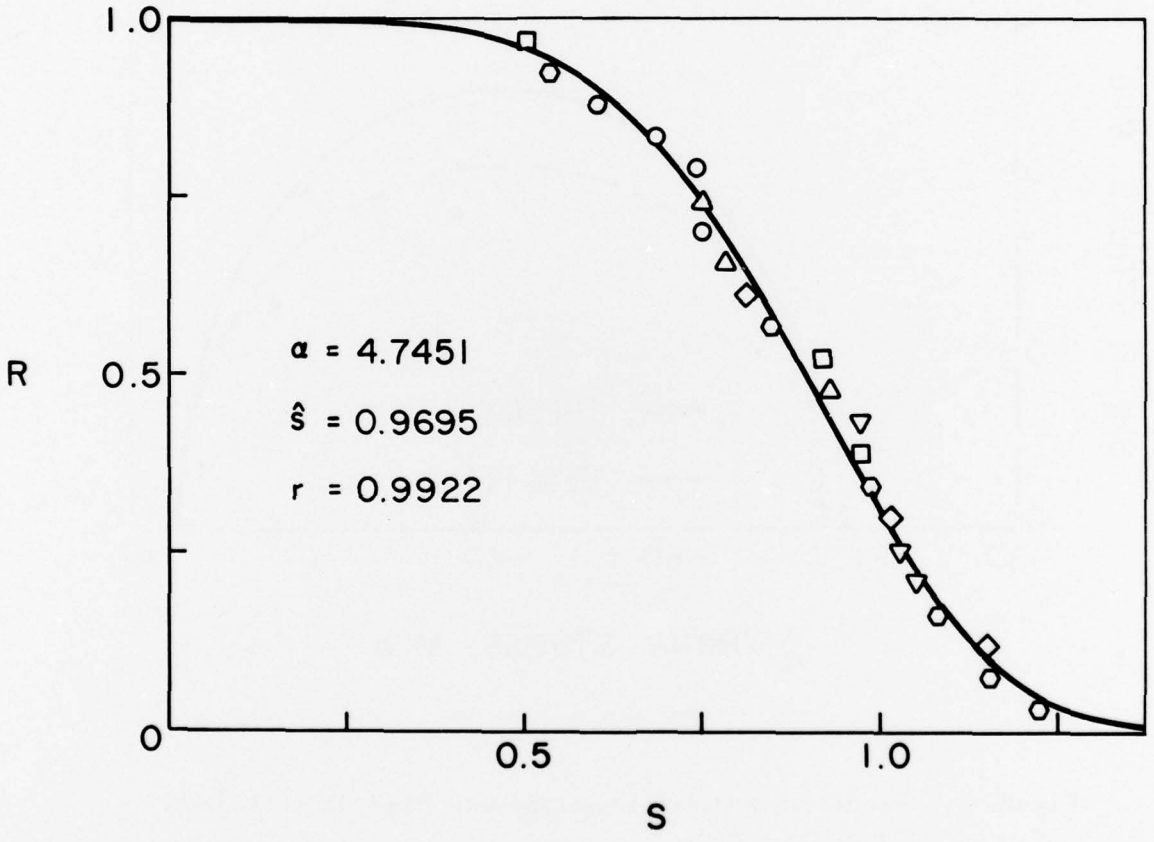

Figure 4. Distribution of s Based on Censored Data.

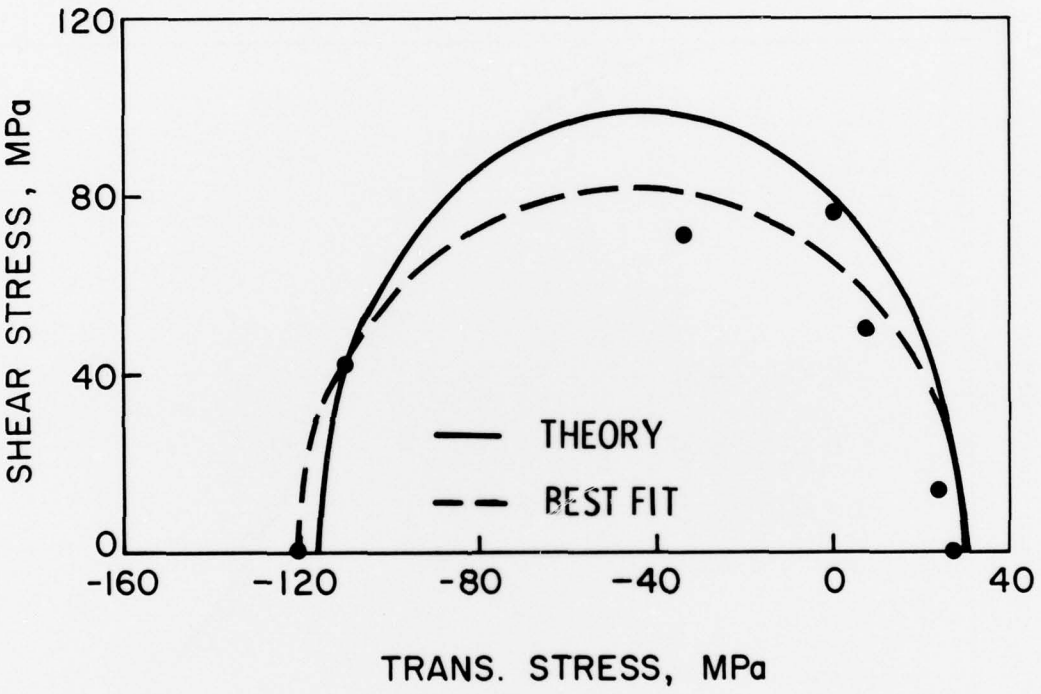

Figure 5. Predicted Failure Envelope and Experimental Data for Short Tubes.

☆U.S.Government Printing Office: 1979 — 657-002/343